ChemPubSoc Europe

DOI: 10.1002/cphc.201900538

CHEMPHYSCHEM Articles

Molecular Electron Density Distribution and X-Ray Diffraction Patterns of Smectic A Liquid Crystals – A Simulation Study

Christian Haege,[a] Stefan Jagiella,[a] and Frank Giesselmann*[a]

X-ray diffraction (XRD) is one of the most important methods to assess the long-range translational order in smectic A (SmA) liquid crystals. Nevertheless, the knowledge about the influence of the molecular electron density distribution (MEDD) on the XRD pattern is rather limited because it is not possible to vary the orientational order, the translational order and the MEDD independently in an experiment. We here present a systematic simulation study in which we examine this effect and show that the MEDD indeed has a major impact on the general appearance of the XRD pattern. More specifically, we find that the smectic layer peaks and the intensity ratios thereof strongly depend on the width of the MEDD. The classic approach by Leadbetter *et al.* to determine the smectic translational order parameter Σ from XRD intensities works if the MEDD is quite narrow. In all other cases the influence of the MEDD has to be taken into account.

1. Introduction

All liquid crystalline phases have a certain degree of orientational and, in the case of smectic liquid crystalline phases, translational order. While the presence of orientational order distinguishes the nematic from the isotropic phase, the presence of translational order distinguishes the smectic phases from the nematic phase. Anisotropic molecules that form a nematic or smectic A (SmA) phase have long range orientational order, meaning that the molecules align roughly parallel. The preferred direction is called the director **n**. While the molecular positions in a nematic phase are disordered, the averaged positions of the molecules in a SmA phase reside on equidistant planes such that the molecules form a 1D stack of 2D fluid layers along the layer normal **k**. Since in a 1D system thermal fluctuations destroy true long range order, the translational order in a SmA phase is considered as quasi-long range.[1] In all directions perpendicular to the layer normal **k**, the molecular positions show no long range translational order and in the case of a SmA phase, the layer normal **k** and the director **n** coincide. The distance between the layers is d and the angle between a molecules long axis and the director **n** is called β. The projection of a center of a molecule on the layer normal is denoted by z. A schematic drawing of a smectic A phase is shown in Figure 1.

The orientational and translational distributions of a SmA phase are often quantified by single values: The orientational order can be quantified by the orientational order parameter $S_2 = 3\langle\cos^2\beta\rangle / 2 - 1/2$. ($S_2 = 0$ for a orientationally disordered isotropic phase and $0 < S_2 < 1$ for a liquid crystalline phase.) The translational order can be described with the translational order parameter $\Sigma = \langle\cos 2\pi z/d\rangle$. ($\Sigma = 0$ for an nematic phase and $0 < \Sigma < 1$ for a smectic phase.) The mixed order parameter σ is used to describe correlations between orientational and translational order. It is given by $\sigma = \langle\cos(2\pi z/d) \cdot (3\langle\cos^2\beta\rangle / 2 - 1/2)\rangle$ (and for a SmA phase $0 < \sigma \leq \Sigma$).[2–4]

One of the most important methods to investigate the order of a liquid crystalline phase is X-ray diffraction.[4–15] The diffraction pattern of an aligned SmA phase exhibits two sets of intensity maxima. The diffuse and broad wide angle maxima correspond to the mean short distance of molecular centers. The peak's width in q is due to the lack of translational long range order perpendicular to **k**, while its width in χ is the consequence of a broad orientational distribution (distribution of angles β). The smectic layers give rise to intense Bragg-like small angle peaks (henceforth called the smectic layer peaks), which are rotated by 90° to the wide angle peaks. A schematic 2D XRD pattern of a SmA phase is shown in Figure 2.

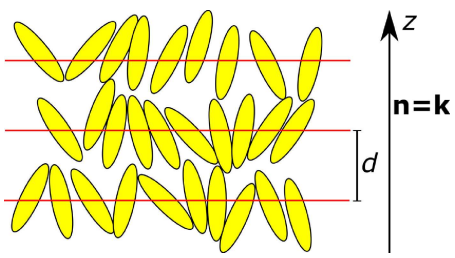

Figure 1. Schematic drawing of a smectic A phase. The layers are separated by distance d and the preferred direction of the molecules is given by the director $\mathbf{n} = -\mathbf{n}$, which coincides with the layer normal $\mathbf{k} = -\mathbf{k}$. For every molecule there is one angle β between its long axis and the director **n**, and a projected coordinate z that gives the projection of the molecular center on the layer normal **k**. The phase has quasi-long range translational order in direction of **k**, whereas the order is only short range perpendicular to **k**.

[a] C. Haege, Dr. S. Jagiella, Prof. Dr. F. Giesselmann
Institute of Physical Chemistry
University of Stuttgart
Pfaffenwaldring 55, 70569 Stuttgart (Germany)
E-mail: f.giesselmann@ipc.uni-stuttgart.de

Supporting information for this article is available on the WWW under https://doi.org/10.1002/cphc.201900538

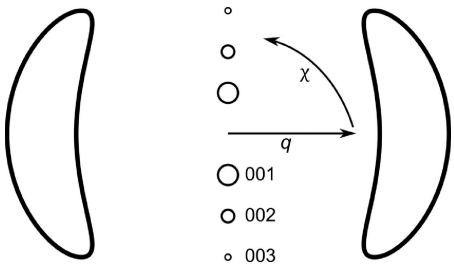

Figure 2. Schematic 2D XRD pattern of a SmA phase. The 2D XRD pattern has two broad wide angle peaks (on the equator) due to scattering from the fluid intra-layer correlations the molecules. The smectic layer peaks labeled 001 to 003 are the result of Bragg-like scattering of the layers.

While the validity of methods to extract information about the orientational order of a liquid crystal has been discussed[6–8,12] the validity of methods that extract information about the translational order is still an open question. In general, the X-ray intensity $I(\mathbf{q})$ is proportional to the structure factor $S(\mathbf{q})$ and the form factor $F^2(\mathbf{q})$ in the sample volume ($I(\mathbf{q}) \propto F^2(\mathbf{q}) \cdot S(\mathbf{q})$). It is not possible to separate the effect of the structure factor and the form factor in an experiment, hence certain assumptions have to be made about the form factor, when extracting data from an XRD pattern. For example, Leadbetter *et al.* either use a model for the structure factor of a smectic layer[9,13] or assume the MEDD to be a point at the molecular center.[11,14] They write the intensity I_{00l} of the l-th layer peak as

$$I_{00l} = C\Sigma_l^2 \langle F_{00l} \rangle^2, \tag{1}$$

with the structure factor F_{00l} of a perfect layer, a constant C and the l-th translational order parameter $\Sigma_l = \langle \cos 2\pi l z/d \rangle$. By assuming Gaussian out-of-layer fluctuations of the molecular center with coordinate z along $\mathbf{k}$, the translational order parameter can thus be written as

$$\Sigma_l = \exp(-2\pi^2 l^2 \langle z^2 \rangle / d^2), \tag{2}$$

and therefore

$$\Sigma_l = \Sigma^{l^2}. \tag{3}$$

Here $\langle z^2 \rangle$ is the mean square displacement of the molecular centers in the direction of $\mathbf{k}$. By assuming that F_{00l} is constant for all l, the translational order parameter can be written as

$$\Sigma = \left(I_{002}/I_{001} \right)^{\frac{1}{6}}. \tag{4}$$

Several other approaches to solve the problem of the translational order parameter have been made: Zannoni et al.[15] present a more direct procedure where the molecular form factor is obtained from atomistic simulations and atomic form factors. They also discuss the neglection of mixed orientational-positional contributions to the intensity of the layer peaks and point out that it is difficult to find the proportionality factors between the intensity of the layer peaks and the translational order parameter. In further attempts Leadbetter et al.[13] and Alexander et al.[5] use the intensities from different neutron and X-ray scattering experiments to model the structure factor of a smectic layer and to determine the translational order parameter. These approaches have the problem that the influence of the actual molecular form factor on the XRD pattern is either approximated or not taken into account. To address this fundamental problem, we present a simulation approach, in which *different* molecular electron density distributions (and therefore different molecular form factors) are used to calculate *different* 2D XRD patterns from the same simulation snapshot. With these XRD patterns, we can directly show what effect changing the molecular electron density distributions (MEDD) has on the intensities of a XRD pattern. We find that the intensity ratios I_{002}/I_{001} of the smectic layer peaks are higher when the aspect ratio of the MEDD is lower. This leads to an underestimation of the translational order parameter Σ when the MEDD is broader. We show that the Leadbetter method[9,11] can be improved if the MEDD is convolved with the distribution of molecular centers $f(z)$ along the layer normal.

2. Simulation Model and Procedure

2.1. Simulation Model

Smectic A phases are simulated using ESPResSo[16] and the Gay-Berne[17] (GB) potential. The dimensions of the GB particles are set to a fixed aspect ratio of 4.

The McMillan[3] model is used to calculate orientational and translational distributions. A McMillan distribution gives the probability $p(\beta, z)$ of finding a molecule at a certain position z along the layer normal, while having a certain angle β to the director. Therefore, a McMillan distribution has a fixed value for the translational, mixed, and the orientational order parameter. The simulations are set up to follow the calculated McMillan distribution. During equilibration the particles are neither allowed to rotate (i.e. change β) nor allowed to translate along the layer normal (change z). All other degrees of freedom are allowed to relax in the molecular dynamics (MD) simulation. Hence, the resulting simulation snapshot represents an energy minimum configuration which follows the underlying McMillan distribution. In this study, McMillan distributions of SmA phases are used and the order parameters are in the following range: $S_2 = 0.75 - 0.93$, $\sigma = 0.4 - 0.85$ and $\Sigma = 0.48 - 0.91$.

Details about the McMillan distributions, the simulation procedure and model can be found in the supporting information.

In order to be able to calculate *different* 2D XRD patterns from the same simulation snapshot, *different* MEDDs are defined. The MEDD used in this study is defined by a molecular electron density ellipsoid inside of the ellipsoidal GB particle. While the semi-minor axes of the molecular electron density ellipsoid in the $x'y'$-plane is fixed to 1/3 (in units of reduced length), the semi-major in the z'-direction (denoted ζ) is

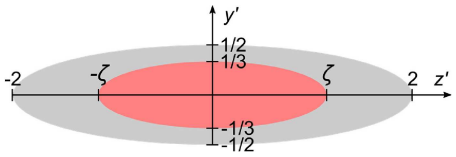

Figure 3. Schematic view of the MEDD (red) inside the GB particle (grey). The geometry of the MEDD is fixed, except for its width (in comparison to the molecular length), which is specified by the semi-major axis ζ in the direction of z' of the long axis of the GB particle.

variable. A 2D schematic of this definition can be seen in Figure 3.

The overall electron density distribution of a snapshot is represented by a regular grid.[12] Inside of the molecular electron density ellipsoid every point of the overall grid is set to a value of 1, while every other point of the overall electron density distribution grid is set to 0.

2.2. Calculation Procedure

The overall 2D XRD calculation can be summarized in three steps:

1. Set the SmA phase according to the underlying McMillan distribution and equilibrate it to get a minimal energy structure that follows that particular McMillan distribution.
2. Inscribe the MEDD described above into the GB particles.
3. Calculate the 2D XRD pattern.

Calculation of 2D X-ray diffraction patterns from the simulations are done using our previously described method[12] with 512 electron density grid points in the x, y and z directions. The cuts of the 3D structure factor are done with an Ewald sphere of reduced wavelength $\lambda^* = 0.077$ and the incident beam orthogonal to the director. The 2D XRD patterns of the last 10 snapshots of a simulation are added to achieve a better signal to noise ratio.

Using this simulation model and calculation procedure has the advantage of a realistic orientational and translational distribution. At the same time, the MEDD can be changed with the semi-major axis ζ between calculations. This model does not allow us to calculate XRD patterns from actual molecules, but it allows for a general assessment of the influence of the MEDD on the XRD pattern.

3. Results and Discussion

In Figure 4b-d three different MEDD (on the left) and their corresponding 2D XRD patterns (on the right) can be seen. All three 2D XRD patterns are calculated from the same simulation snapshots. Figure 4a shows an experimental diffraction pattern of 5-Octyl-2-(4-hexyloxyphenyl-)pyrimidine in the SmA phase (on the right) and the corresponding MEDD of the molecule in the all-trans conformation projected on its long axis (on the left). It can directly be seen that the MEDDs differ significantly.

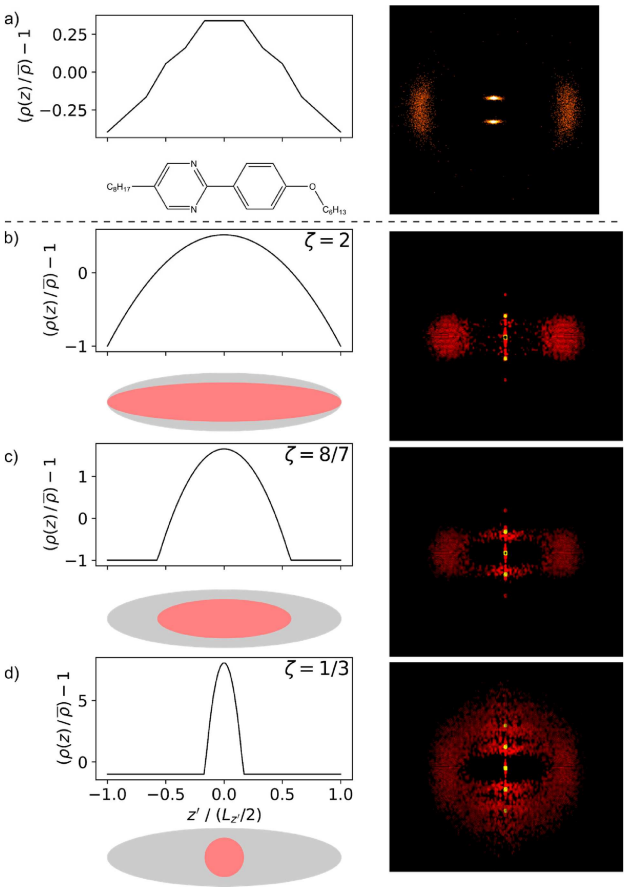

Figure 4. On the left: Molecular electron densities projected on the long axis of a typical molecule and the ellipsoidal (and spherical) electron densities as incorporated in the GB-particles. The lengths are shown in units of $L_{z'}/2$, where $L_{z'}$ is the length of the molecule or GB-particle in the z'-direction. Under the plots the corresponding shapes are shown. On the right: diffraction patterns that correspond to the molecular electron densities on the left. **a)** Molecular electron density for 5-Octyl-2-(4-hexyloxyphenyl)-pyrimidine in the all-trans conformation and a 2D XRD of the substance in the SmA phase at $T = 55$ °C. Calculating the 2D XRD pattern from this MEDD gives roughly the same pattern as shown in Figure b. **b-d)** Molecular electron density of ellipsoidal shape (red) in a GB-particle. The electron density ellipsoids have semi-major axis $\zeta = 2, \frac{8}{7}, \frac{1}{3}$ from top to bottom. On the right the corresponding diffraction patterns calculated from the same simulation (order parameters $S_2 = 0.82$, $\sigma = 0.59$ and $\Sigma = 0.68$) are shown.

Therefore, it is no surprise that the 2D XRD patterns also differ. Moreover, it can be seen that the intensities of the smectic layer peaks vary in Figure 4b–d. This effect and its implications on the calculation of the translational order parameter Σ are now discussed.

The integrated intensities of the layer peaks are analyzed by calculating the intensity ratio I_{002}/I_{001}. The data show that the intensity ratio increases with increasing translational order parameter. The intensity ratio also increases with decreasing radius ζ, which means that the intensity ratio is higher when the MEDD is more narrow. The intensity ratio I_{002}/I_{001} for different order parameters and MEDDs can be seen in Figure 5.

This result implies that any procedure that uses the intensity ratios of the smectic layer peaks should include the MEDD in some way. The implications are discussed exemplarily in the

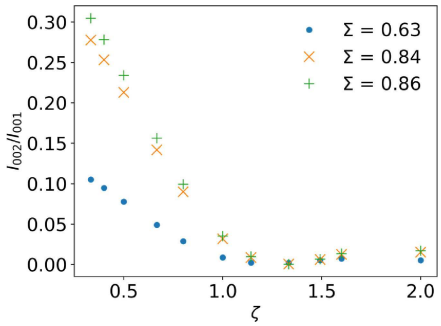

Figure 5. Intensity ratio I_{002}/I_{001} of the smectic layer peaks of the calculated 2D XRD patterns for different values of the semi major axis ζ of the MEDDs. Order parameters: $S_2 = 0.80$, $\sigma = 0.54$ and $\Sigma = 0.63$, $S_2 = 0.89$, $\sigma = 0.75$ and $\Sigma = 0.84$ and $S_2 = 0.9$, $\sigma = 0.77$ and $\Sigma = 0.86$.

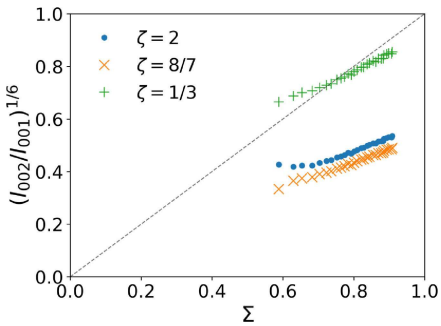

Figure 6. The 6th root of ratio of the integrated intensity of the second and first small angle peak calculated from 2D XRD patterns with different MEDDs (different semi major axes ζ – (see also Figure 3)) plotted with respect to Σ. Σ is directly calculated from the McMillan distributions. The dotted line represents the expected trend according to equation (4).

are calculated with Σ known from the underlying McMillan distributions and the layer separation d as taken directly from the simulations. The root mean square displacement $\langle z^2 \rangle$ is calculated via equation (2), and with $\langle z^2 \rangle$ known, the distribution of molecular centers along **k** is calculated by including the smectic layer positions z_L. The Gaussian form of the distribution is then given by

$$f(z) = \frac{1}{\sqrt{2\pi\langle z^2 \rangle}} \cdot \exp\left(-\frac{(z - z_L)^2}{2\langle z^2 \rangle}\right). \tag{5}$$

Here the layer positions are given by $z_L = d \cdot [\lfloor z/d \rfloor + 1/2]$.

An example of the Gaussian form of the distribution of molecular centers along **k** according to equation (5) and electron density plots of the simulation for different semi-major axes ζ can be seen in Figure 7. The MEDD that represents the

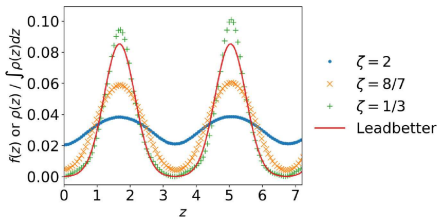

Figure 7. z-projection of the electron density distribution for order parameters $S_2 = 0.82$, $\sigma = 0.59$ and $\Sigma = 0.68$ of the first two layers and the Gaussian form of the distribution of molecular centers along **k** as assumed by Leadbetter *et al.*[9,11] The data that is marked "Leadbetter" is calculated via equation (5) with different values of z_L (for every layer), $\Sigma = 0.68$ and $d = 3.36$. The data with different semi-major axis ζ are calculated from the overall electron density distribution of the last simulation snapshot (snapshot 500000).

next part by looking at the Leadbetter method[9,11] for extracting translational order parameters from intensity ratios.

When using X-ray diffraction to calculate Σ, Leadbetter assumes a Gaussian shape of the distribution of molecular centers along **k** to calculate the translational order parameters of smectic phases. From their assumption one can derive equation (4). Plotting the intensity ratio $(I_{002}/I_{001})^{1/6}$ over the translational order parameter directly taken from the McMillan distributions reveals that equation (4) is correct in the case of narrow MEDDs. If the MEDDs is broad (large ζ), the method underestimates the translational order parameter. In Figure 6 such plot can be seen. It is clear that only in the case of the narrow, spherical MEDD ($\zeta = 1/3$), the expected result is obtained.

To understand the results seen in Figure 6 it is useful to calculate the electron density wave along the layer normal (*e.g.* along z) and to compare it with the positional distribution that is used by Leadbetter *et al.*[9,11]. From the simulations the electron density along the z-direction is directly calculated by projecting all points of the electron density grid on the z-axis and summing of the electron density for every projected value. To compare the electron density plots to the Gaussian distribution assumed by Leadbetter, the Gaussian distributions Leadbetter assumption[9,11] of a Gaussian distribution the most, is the narrow one with $\zeta = 1/3$. This is in agreement with the result presented in Figure 6 where it can be seen, that the intensity ratios from the spherical MEDD are closest to the expected trend (equation (4)).

While it has been explained above why the spherical MEDD is closest to the expected result, this still leaves one question: why do the results from broader MEDDs ($\zeta = 8/7, 2$) underestimate the translational order parameter Σ? The answer to this question lies in the assumptions made by Leadbetter *et al.*[9,11] Leadbetter[9,11] neglects the exact MEDD and proposes a Gaussian form of the distribution of molecular centers along the layer normal **k**. While the latter is reasonable, neglecting the actual MEDD leads to a systematic error. This can be shown by calculating the convolutions of the Gaussian distribution of molecular centers along the layer normal **k** and the MEDD. Comparing the convolutions to the overall electron density distribution of a simulation snapshot should give the same result, if the MEDD is not to be neglected.

To calculate the convolution two steps are necessary. First, an equation describing the MEDD is needed. The electron density is the same at every point in the molecular electron density ellipsoid (see also section "Simulation model") and the

number of electron density grid points per volume element is the same everywhere. Therefore, the area of a cut of the ellipsoid is directly proportional to the electron density at the position of the cut. Hence, it is reasonable to describe the electron density by calculating the area of a cut of a rotated ellipsoid, where the ellipsoid has been rotated around the *x*-axis by an angle α and the cutting layer has position *z* along the layer normal $\mathbf{n}_L = (0,0,1)^T$. The MEDDs used in the simulations are uniaxial, thus one rotation angle is enough to describe the MEDD, and it does not matter if the ellipsoid is rotated around the *x*- or the *y*-axis. With the help of the equations in Ref.[18] we obtain the following equation for the cutting area (see also: supporting information),

$$A(z,\alpha) = \begin{cases} \pi abc \cdot \frac{\left(b^2\sin^2\alpha + c^2\cos^2\alpha - z^2\right)}{\left(b^2\sin^2\alpha + c^2\cos^2\alpha\right)^{\frac{3}{2}}} & \text{if } z^2 \le b^2\sin^2\alpha + c^2\cos^2\alpha \\ 0 & \text{else.} \end{cases} \quad (6)$$

Second, the convolution is calculated. To calculate the convolution, the semi-axes *a*, *b* and *c* in equation (6) are selected according to the MEDD and the rotation angle is set to be the average angle $\langle\beta\rangle$ of the GB particles to the layer normal. The electron density distribution of a layer is given by convolving equation (5) and (6) according to

$$\frac{\rho_{e,\text{layer}}(z)}{\int \rho_{e,\text{layer}}(z)dz} \approx \frac{\sum_i f(z_i)\cdot A(z-z_i,\langle\beta\rangle)}{\sum[\ \sum_i f(z_i)\cdot A(z-z_i,\langle\beta\rangle)\ ]\Delta z}. \quad (7)$$

Comparison of the calculated convolutions to the overall electron density distribution of the last simulation snapshot shows that both are in perfect agreement. Three examples of the Gaussian distribution as assumed by Leadbetter *et al*,[9,11] the overall electron density distribution of the last simulation snapshot, and the convolutions calculated according to equation (7) can be seen in Figure 8.

This shows, that the intensity ratios calculated with the narrow MEDD ($\zeta = 1/3$) are in agreement with Leadbetter's method[9,11] (see Figure 6). We could also show that the assumed Gaussian distribution[9,11] and the overall electron density distribution of a simulation snapshot coincide in this case (see Figure 7), and therefore the correct trend is obtained. When using broad MEDDs (*e.g.* $\zeta = 8/7, 2$) a systematic underestimation of Σ is the result. To better understand this, convolutions of the assumed Gaussian distribution[9,11] and the MEDD are calculated. The agreement of the convolutions and the electron density distribution of the last simulation snapshot (see Figure 8) show, that the correct MEDD has to be taken into account when the intensities of an 2D XRD pattern are used for further calculations.

4. Discussion

Our results have certain implications for the general assessment of smectic order from XRD patterns. Strictly speaking, the general opinion that a high degree of smectic 1D translational order is indicated by the presence of strong higher order layer peaks is only valid in those cases where the mesogenic molecules exhibit a sharp peak in their MEDDs. In these cases the actual MEDD comes close to the δ-peaked MEDD assumed in the original paper by Leadbetter[9,11] and the smectic order parameter Σ can be estimated from the intensity ratios I_{002}/I_{001}. In practice, this condition of a narrow-peaked MEDD can be approached if the mesogens contain electron-rich heteroatoms (or groups) in their molecular structure. Examples are the siloxane[19,20] or carbosilane[21] terminated mesogens of many de Vries-type smectics[4] or ionic smectic liquid crystals[22] with heavy electron-rich counterions such as sulfate or bromide anions.

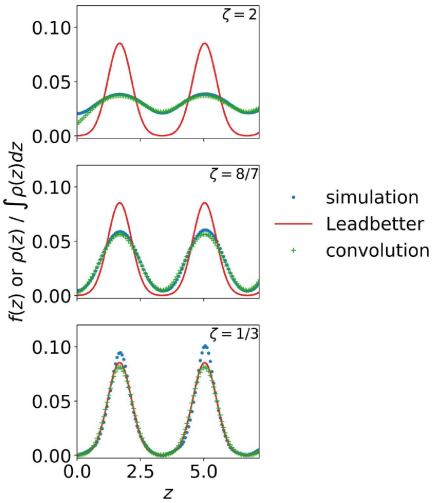

Figure 8. *z*-projections of the electron density distribution for order parameters $S_2 = 0.82$, $\sigma = 0.59$ and $\Sigma = 0.68$ of the first two layers of the simulation. The data marked "simulation" are the (normalized) sum of the calculated snapshot electron density along the layer normal of the last simulation snapshot (snapshot 500000). The MEDDs used during the calculation have semi-axes $\zeta = 2, \frac{8}{7}, \frac{1}{3}$ from top to bottom. The data that are labelled "Leadbetter" are calculated via equation (5) with different values of z_L (for every layer), $\Sigma = 0.68$ and $d = 3.36$. The data labeled "convolution" are the data marked "Leadbetter" (equation (5)) that have been convolved with equation (6) according to equation (7). The average angle of the particles to the layer normal is selected (here: $\langle\beta\rangle \approx 17°$) as the rotation angle. The semi-axes *a*, *b* and *c* in equation (6) are selected according to the semi-axes of the ellipsoidal particle electron density distributions.

Figure 9 schematically depicts the situation in the SmA phase of siloxane-terminated mesogens such as the one shown in Figure 10. In the SmA phase, the hydrocarbon parts of the mesogen segregate from the terminal siloxane segments such that they form siloxane-rich sublayers between the partial bilayers of the mesogenic cores (Figure 9, left). This nanosegregation[20] of the electron-rich siloxane segments gives rise to narrow peaks in the SmA electron density wave $\rho_e(\mathbf{k})$ as shown in Figure 9, right. The Fourier transform of $\rho_e(\mathbf{k})$ in Figure 9 requires substantial contributions from higher harmonics of the fundamental electron density wave. Since the XRD intensities of the (00*l*) layer peaks basically probe the (squared) amplitudes of the *l*-th harmonics in the Fourier transform of the SmA electron density wave,[23] intense higher-order layer

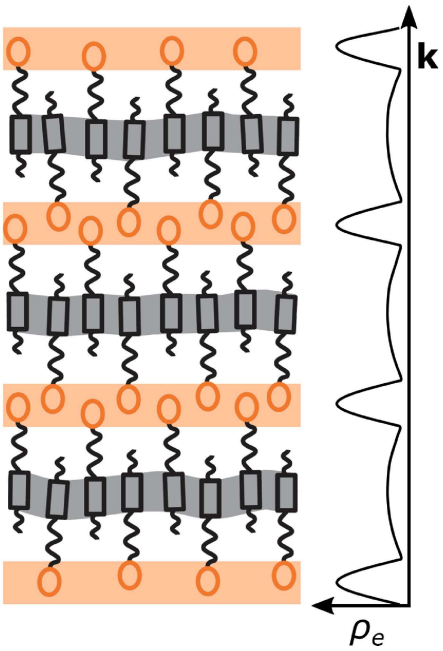

Figure 9. Left: Schematic drawing of a layered SmA structure with nanosegregation between electron-rich end groups (orange) and mesogenic cores (grey). Right: Resulting electron density wave $\rho_e(\mathbf{k})$ along the layer normal **k** of the SmA phase. The nanosegregation of electron-rich molecular segments leads to sharp peaks in $\rho_e(\mathbf{k})$.

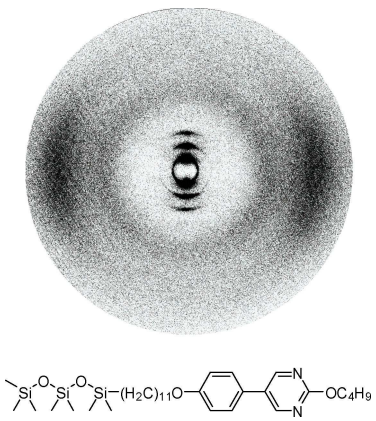

Figure 10. Top: 2D XRD pattern of the nanosegregated SmA phase formed by the mesogen shown below. The diffraction pattern shows intense higher order smectic layer peaks. Bottom: Molecular structure of a trisiloxane-terminated mesogen forming nanosegregated smectic phases of the de Vries-type.[24]

peaks are expected. This is indeed the case as seen in the example depicted in Figure 10. The same considerations apply to the case of ionic smectics where heavy counterions segregate in a similar way into electron-rich sublayers.

If, however the MEDD profile of the mesogen is rather smooth without any sharp peaks or other distinct features, the SmA electron density wave $\rho_e(\mathbf{k})$ is well described by a more or less sinusoidal wave of fundamental period d and, maybe, some very little contributions from higher harmonics of the fundamental wave. Even if the smectic translational order becomes high, the electron density wave along **k** remains almost sinusoidal and thus no intense higher order peaks might be detected in the XRD experiment. An example of such an experimental 2D XRD pattern can be seen in Figure 4a. No higher order peaks are visible. In this case however the absence of higher order layer peaks does not necessarily mean that the smectic 1D translational order is exceptionally low.

5. Conclusions

In this paper we show that the intensity ratios of smectic layer peaks of X-ray diffraction patterns strongly depend on the molecular electron density distribution (MEDD). We find that the intensity ratios I_{002}/I_{001} are higher the narrower the MEDD is concentrated along the direction of the long axis of the molecule.

The consequence of this result on the calculation of translational order parameters is discussed, using Leadbetter's method[9,11] as an example. The results show that accurate calculations must take the MEDD into account. To be more precise, the SmA electron density wave $\rho_e(\mathbf{k})$ along the layer normal **k** should be deconvolved with the MEDD and the translational order parameter Σ calculated from the deconvolution result.

We also discuss the implications of our results on the general assessment of smectic translational order from experimental XRD patterns. In those cases where the MEDD exhibits sharp peaks in the electron density (namely mesogens containing electron-rich heteroatoms), high 1D translational order of the mesogens also leads to sharp peaks in the SmA electron density wave and thus to the appearance of intense higher-order diffraction peaks in the XRD experiment. In these cases the presence and the intensities of the higher-order layer peaks are at least a reliable qualitative proof of high smectic order. In other cases where the MEDD is smooth and without any distinct peaks, the SmA electron density wave is essentially of sinusoidal shape and higher order layer peaks thus remain very weak regardless whether or not smectic translational order of the SmA phase is high.

Acknowledgements

We thank Peter J. Collings for many helpful discussions. We further thank Andreas Bogner for the 2D XRD pattern in Figure 10 and parts of Figure 9.

Conflict of Interest

The authors declare no conflict of interest.

Keywords: liquid crystals · molecular dynamics · order parameter · smectic translational order · X-ray diffraction

[1] J. Als-Nielsen, J. D. Litster, R. J. Birgeneau, M. Kaplan, C. R. Safinya, A. Lindegaard-Andersen, S. Mathiesen, *Phys. Rev. B* **1980**, *22*, 312.
[2] W. L. McMillan, *Phys. Rev. A* **1972**, *6*, 936.
[3] W. L. McMillan, *Phys. Rev. A* **1971**, *4*, 1238.
[4] J. P. F. Lagerwall, F. Giesselmann, *ChemPhysChem* **2006**, *7*, 20.
[5] G. G. Alexander, S. M. King, R. M. Richardson, H. Zimmermann, *Liq. Cryst.* **2010**, *37*, 961.
[6] M. T. Sims, L. C. Abbott, R. M. Richardson, J. W. Goodby, J. N. Moore, *Liq. Cryst.* **2018**, *371*, 11.
[7] P. Davidson, D. Petermann, A. M. Levelut, *J. Phys. II* **1995**, *5*, 113.
[8] D. M. Agra-Kooijman, M. R. Fisch, S. Kumar, *Liq. Cryst.* **2017**, *45*, 680.
[9] A. J. Leadbetter, E. K. Norris, *Mol. Phys.* **1979**, *38*, 669.
[10] N. Kapernaum, F. Giesselmann, *Phys. Rev. E* **2008**, *78*, 62701.
[11] A. J. Leadbetter, P. G. Wrighton, *J. Phys. Colloq.* **1979**, *40*, C3-234.
[12] F. Jenz, S. Jagiella, M. A. Glaser, F. Giesselmann, *ChemPhysChem* **2016**, *17*, 1568.
[13] A. J. Leadbetter, J. C. Frost, J. P. Gaughan, G. W. Gray, A. Mosley, *J. Phys. France* **1979**, *40*, 375.
[14] A. J. Leadbetter, *Structural studies of nematic, smectic A and smectic C phases. The molecular physics of liquid crystals.* p. 285, Acadamic Press, London, **1979**.
[15] M. F. Palermo, A. Pizzirusso, L. Muccioli, C. Zannoni, *J. Chem. Phys.* **2013**, *138*, 204901.
[16] a) L. Verlet, *Phys. Rev.* **1967**, *159*, 98; b) A. Arnold, K. Breitsprecher, F. Fahrenberger, S. Kesselheim, O. Lenz, C. Holm, *Efficient algorithms for electrostatic interactions including dielectric contrasts*, Universität Stuttgart, **2013**; c) A. Arnold, O. Lenz, S. Kesselheim, R. Weeber, F. Fahrenberger, D. Roehm, P. Košovan, C. Holm in *Lecture Notes in Computational Science and Engineering*, *Vol. 89* (Eds.: M. Griebel, M. A. Schweitzer), Springer, Berlin, Heidelberg, **2013**, pp. 1–23; d) H. J. Limbach, A. Arnold, B. A. Mann, C. Holm, *Comput. Phys. Commun.* **2006**, *174*, 704.
[17] J. G. Gay, B. J. Berne, *J. Chem. Phys.* **1981**, *74*, 3316.
[18] P. P. Klein, *Appl. Math.* **2012**, *03*, 1634.
[19] a) H. Yoon, D. M. Agra-Kooijman, K. Ayub, R. P. Lemieux, S. Kumar, *Phys. Rev. Lett.* **2011**, *106*, 87801; b) J. C. Roberts, N. Kapernaum, Q. Song, D. Nonnenmacher, K. Ayub, F. Giesselmann, R. P. Lemieux, *J. Am. Chem. Soc.* **2010**, *132*, 364.
[20] H. J. Coles, H. Owen, J. Newton, P. Hodge, *Liq. Cryst.* **1993**, *15*, 739.
[21] a) K. M. Mulligan, A. Bogner, Q. Song, C. P. J. Schubert, F. Giesselmann, R. P. Lemieux, *J. Mater. Chem. C* **2014**, *2*, 8270; b) C. P. J. Schubert, C. Müller, A. Bogner, F. Giesselmann, R. P. Lemieux, *Soft Matter* **2017**, *13*, 3307; c) R. A. Reddy, C. Zhu, R. Shao, E. Korblova, T. Gong, Y. Shen, E. Garcia, M. A. Glaser, J. E. Maclennan, D. M. Walba, *Science* **2011**, *332*, 72.
[22] K. Goossens, K. Lava, C. W. Bielawski, K. Binnemans, *Chem. Rev.* **2016**, *116*, 4643.
[23] P. Davidson, A. M. Levelut, M. F. Achard, F. Hardouin, *Liq. Cryst.* **1989**, *4*, 561.
[24] A. Bogner, *Maßgeschneiderte smektische Flüssigkristalle vom ‚de Vries'-Typ. Struktur-Eigenschaftsvariationen in nanosegregierenden Organosiloxanen und Organocarbosilanen*, Universität Stuttgart, **2015**.

Manuscript received: May 27, 2019
Accepted manuscript online: July 30, 2019
Version of record online: August 20, 2019